Influence of Scour Protection on the Vertical Bearing Behaviour of Monopiles in Sand

Li, Qiang; Wang, Xinquan; Gavin, Kenneth; Jiang, Shengxiang ; Diao, Hongguo ; Wang, Kangyu

DOI
10.3390/w16020215

Publication date
2024

Document Version
Final published version

Published in
Water

water

MDPI

Article

Influence of Scour Protection on the Vertical Bearing Behaviour of Monopiles in Sand

Qiang Li [1,2], Xinquan Wang [1,3,4,*], Kenneth Gavin [5], Shengxiang Jiang [6], Hongguo Diao [1,3,4] and Kangyu Wang [7]

1 Department of Civil Engineering, Hangzhou City University, Hangzhou 310015, China; qiangli1991@outlook.com (Q.L.); diaohg@zucc.edu.cn (H.D.)
2 PowerChina Huadong Engineering (Shenzhen) Corporation Limited, Shenzhen 518100, China
3 Key Laboratory of Safe Construction and Intelligent Maintenance for Urban Shield Tunnels of Zhejiang Province, Hangzhou 310015, China
4 Zhejiang Engineering Research Center of Intelligent Urban Infrastructure, Hangzhou 310015, China
5 Faculty of Civil Engineering and Geosciences, Delft University of Technology, 2628 CN Delft, The Netherlands; k.g.gavin@tudelft.nl
6 PowerChina Huadong Engineering Corporation Limited, Hangzhou 310014, China; jiang_sx@hdec.com
7 School of Civil Engineering, Zhejiang University of Technology, Hangzhou 310014, China; kangyuwang@zjut.edu.cn
* Correspondence: wangxq@zucc.edu.cn; Tel.: +86-137-5715-8022

Abstract: Extensive studies have been performed on the effectiveness of scour protection against scour erosion progression. But there is little research to date evaluating the effect of scour protection on vertical resistance behaviour of monopile foundations. This paper investigates the influence of scour protection on the vertical loading behaviour of monopiles installed in sand using centrifuge tests and finite element analysis (FEA). Four scour protection widths (1*D*, 2*D*, 3*D*, 4*D*; where *D* is the pile diameter) and three scour protection thicknesses (1 m, 2 m, 3 m) were modelled on a pile with a slenderness ratio (*L*/*D*) of five. In the FEA, the scour protection mechanism was modelled using two strategies, namely the 'stress method' by applying stress and the 'material method' by applying virtual material on the seabed surface around the pile. Outcomes between these two strategies were compared, and the contact coefficient δ used in the 'material method' for describing the contact effectiveness of the overlaying scour protection material with the pile structure was introduced, providing a more scientific and accurate calculation reference for engineering applications. The results indicated that the vertical capacity of monopiles could be increased by 5% to 23% by adopting the scour protection measure, depending on the scour protection width and scour protection thickness.

Keywords: piles and piling; scour protection; vertical resistance; finite element methods; centrifuge modelling

Citation: Li, Q.; Wang, X.; Gavin, K.; Jiang, S.; Diao, H.; Wang, K. Influence of Scour Protection on the Vertical Bearing Behaviour of Monopiles in Sand. *Water* **2024**, *16*, 215. https://doi.org/10.3390/w16020215

Academic Editor: Helena M. Ramos

Received: 28 November 2023
Revised: 15 December 2023
Accepted: 5 January 2024
Published: 7 January 2024

1. Introduction

Offshore wind turbines (OWTs) are usually designed with a lifetime of 20 to 25 years. The monopile foundation plays a dominant role in the offshore wind industry, accounting for 81% of all the foundation installations of OWTs, especially in Europe [1]. In the case that the older generation of OWTs is running out of its lifetime, it should be repowered or replaced with new and efficient turbines out of economic and environmental considerations [2].

The OWTs founded on a monopile foundation can be repowered by isolating the turbine from the grid and de-energizing it. Afterwards, outdated blades, nacelles, and towers are removed and dismantled [3,4]. Updated blades, nacelles, and towers, which are usually newly designed with advanced material and a larger size and weight, could be installed on the remaining monopile foundation. What calls for special attention is that

prior to installation, the monopile foundation needs to be re-assessed on the structural health, vertical and lateral capacities, etc., to ensure its safety.

Scouring around the monopile foundation is a well-recognised issue [5–7], which will reduce the foundation embedment and effective stress along the pile, compromising the lateral response of the monopile [8–10]. The scour protection layer, formed by rock armour, rubble filter and other materials, is found to not only compensate for the lost pile lateral resistance by scouring but also increases the lateral resistance of the pile from a proper scour protection design [11]. A typical in-place scour protection laid on the seabed is schematically shown in Figure 1, where D refers to the pile diameter, L refers to the pile (original) embedment length, h refers to the water depth, P_w refers to the scour protection width and P_t refers to the scour protection thickness. Askarinejad et al. [11] presented that a scour protection layer with a diameter five times that of the monopile (5D) and an equivalent surcharge pressure of 15 kPa increases the lateral capacity of the foundation in dense sand by more than 30% and reduces the accumulated lateral deflection by more than 100%.

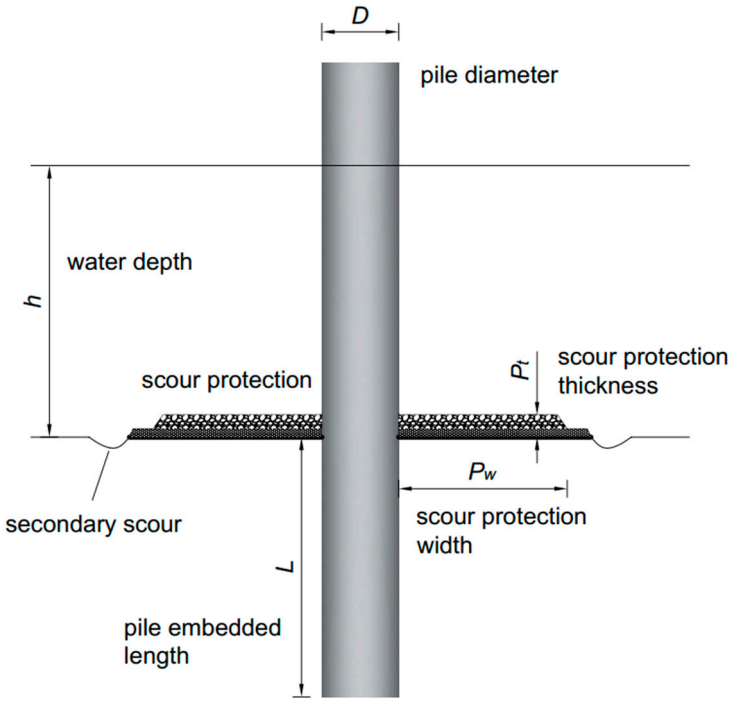

Figure 1. Scour protection in place.

Compared with the increase in lateral loading caused by enlarged blades, nacelle, and tower after the replacement old turbines with new ones, the increase in vertical loading is comparatively not that significant. Enhancing the vertical resistance of the monopile by maintaining and/or upgrading the scour protection could be a possible choice. However, there is little research revealing the effect of the scour protection layer on the vertical loading behaviour of the pile.

In light of these discussions, this research aims to explicitly evaluate the effect of scour protection on the vertical loading behaviour of the monopile by means of centrifuge tests and finite element analysis (FEA). Different parameters were considered, including the scour protection width, scour protection thickness and scour protection application method. In all cases considered, the pile was embedded in homogeneous, dry, dense sand.

2. Centrifuge Modelling

2.1. Model Pile and Soil Characterisation

The experiments were performed using the beam centrifuge at Delft University of Technology [12,13] with a centrifugal acceleration rate of 100× g. An open-ended steel pipe pile with outer diameter of D = 1.8 m and wall thickness of t = 3 cm in prototype size was modelled. The pile had an embedded length of L = 9 m, as well as a slenderness ratio (L/D) of 5, which is widely used in offshore foundations [14,15]. The free length of the pile body can be expressed as $e = 8D$, calculated from the original seabed surface. It is worth noting that the prototype dimensions of the pile were smaller than those used for OWTs in practical construction [16]. Large piles could not be used in this centrifuge due to several boundary effects, e.g., limitation of the centrifuge basket and of the strong box holding the sand specimens. But existing research has shown that results from tests on such a pile could provide useful guidance for field applications thanks to the very favourable slenderness (rigidity) of the simulated pile [17–19].

Dry Geba silica sand with relative density of D_r = 80% was used to form the seabed. The basic properties of Geba sand are summarised in Table 1. The ratio of outer pile diameter to mean particle size of the sand (D/D_{50}) was approximately 164, which was considered large enough to avoid the effect of particle size [16]. The ratio of pile wall thickness to mean particle size of the sand (t/D_{50}) was 9.1, very close to the suggested limiting value of 10 [20,21], allowing the full interaction between the pile annulus and the soil [16].

Table 1. Soil properties of Geba sand [16].

e_{min}	e_{max}	G_s	D_{50} (mm)	C_U	φ'
0.64	1.07	2.67	0.11	1.55	34°

Influence of water was excluded in the experimental trials conducted in this article. This is a simplification and a deviation from the physical environment of offshore pile foundations. However, the presence of water is not expected to alter the behavioural trends of scour protection on pile vertical resistance, rather its presence would lower the effective unit weight of the sand. Similar treatments in centrifuge experiments can be found in Mu et al. [22], Verdure et al. [23], Klinkvort and Hededal [24], LeBlanc et al. [25], Li et al. [26] and Li et al. [8].

2.2. Centrifuge Loading Technique and Test Program

A two-dimensional actuator was used to impose a vertical load on the monopile under displacement-controlled condition in the centrifuge in Geo-laboratory of TU Delft [19], as shown in Figure 2a. Vertical displacement was monitored using a displacement encoder, with an accuracy of 1 × 10^{-2} mm. The two loading arms were connected by a loading bar, with a transition piece installed in the middle and a vertical load cell installed in the end (as shown in Figure 2b), which had a measurement capacity of 5 kN (Model 8431-6005, Burster, Gernsbach, Germany). A loading plate was attached to the bottom of the vertical load cell to transfer the produced vertical load to the pile. The capacity of the vertical load cell was determined upon the loading capacity of the two-dimensional loading system, as well as the force required to jack the pile, as justified from preliminary tests. The enhanced gravitational level was set to 100× g for these reasons, as higher enhanced gravitational level requires a much larger force to jack the pile inflight of such size.

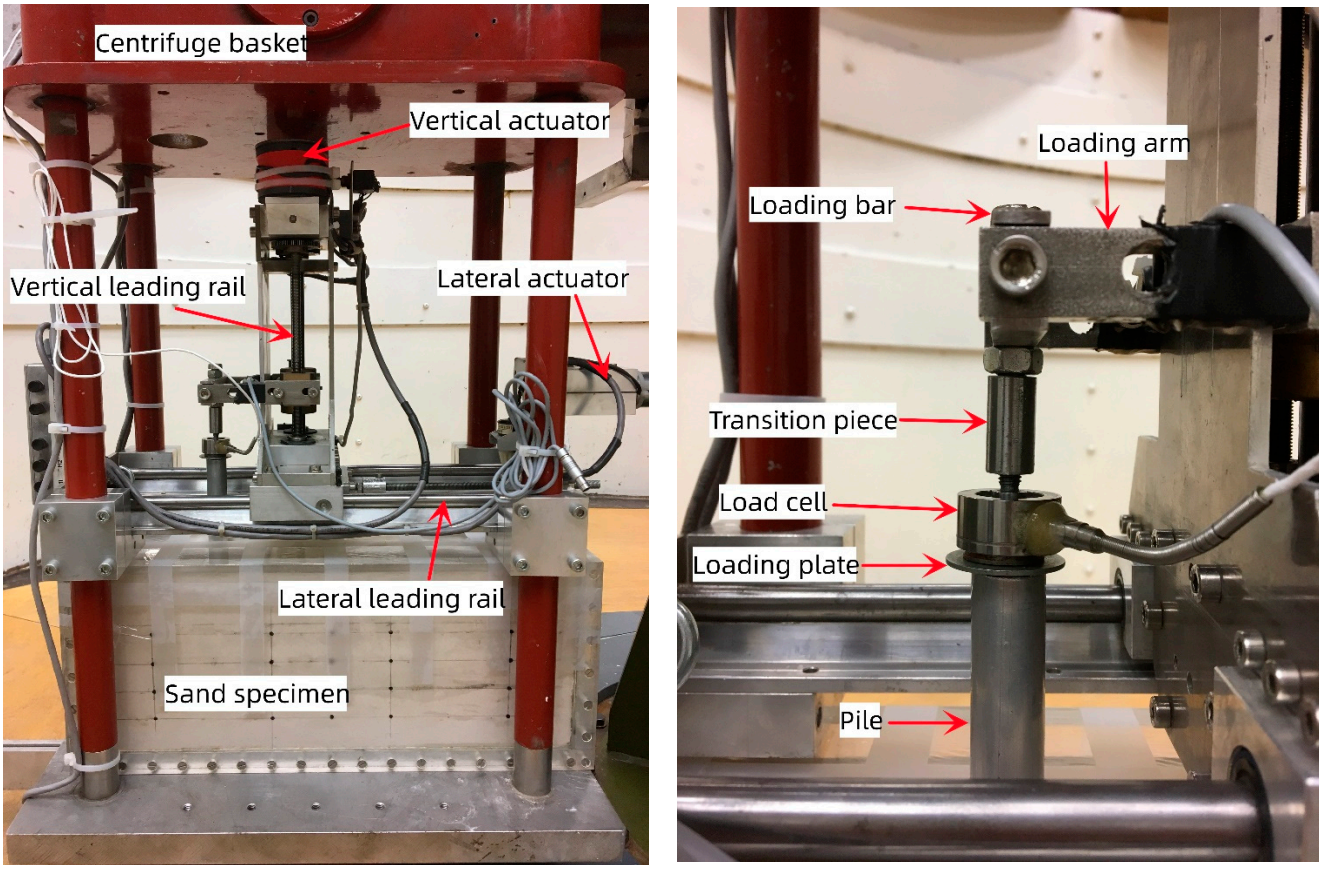

(**a**) (**b**)

Figure 2. (**a**) Two-dimensional loading actuator and (**b**) details of the vertical loading apparatus.

As shown in Table 2, three centrifuge tests were performed in this study: one test in the absence of scour protection and two tests in the presence of scour protection. In the experimental investigation of scour protection geometries, Du [27] has confirmed that the most effective scour protection width should cover the scour hole edge (if no scour protection) for preventing scour development, and this value for a small diameter pile is 3*D*, and for a large diameter pile is 2*D*. Therefore, two different scour protection widths, specifically 2*D* and 3*D*, with an equivalent effective surcharge pressure of 15 kPa, were designed in this study [11,28]. The scour protection layer was formed using Geba sand, by a specially designed sand pouring tube. To be noticed, large stone and gravel is usually combined to establish the scour protection layer in practical engineering applications [29] for the purpose of pore water pressure dissipation and structure stabilization. However, the difference caused by the overall size and particle distribution of scour protection materials on the vertical bearing behaviour of the pile should be minimal as dry sand was used to simulate the seabed in this research.

Table 2. Centrifuge test programme.

Test ID	Soil	Pile Geometry	Scour Protection Width	Scour Protection Pressure
CT-1	Geba sand (D_r = 80%)	D = 1.8 m, L = 5D	0	-
CT-2			2D	15 kPa
CT-3			3D	15 kPa

Each centrifuge test followed the subsequent procedures: (1) the model pile was firstly installed into the seabed by jacking at 1× g; (2) according to the requirements, scour

protection was added on the seabed (or not); and (3) the centrifuge was raised to 100× g, and then, vertical loading was applied to the pile head.

3. Finite Element Analysis

3.1. Mesh Details

In order to reveal the internal mechanism, FEA was performed on PLAXIS 3*D* CE V20. The mesh size is shown in Figure 3. Considering the symmetry of the problem, only half of the pile–soil system was modelled for computational efficiency.

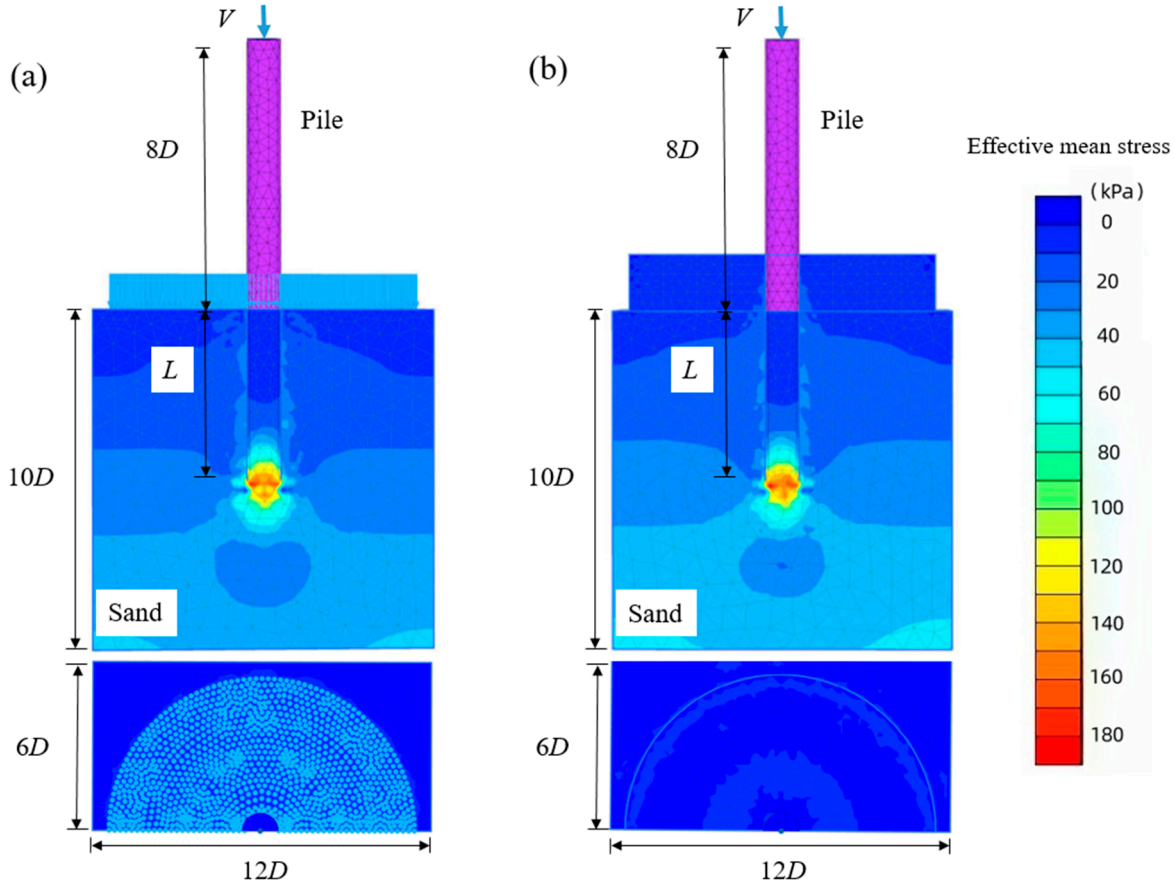

Figure 3. Typical mesh adopted in three-dimensional Finite Element Analysis: (**a**) 'stress method' and (**b**) 'material method'.

The soil domain with 12*D* in length, 6*D* in width and 10*D* in height was used for the simulation of the seabed. These dimensions were large enough to eliminate the boundary effect on the FE solutions based on some trial analyses. The mesh was highly refined in and around the pile and became coarser near the boundary. The lateral boundaries of the seabed were supported by a simplified roller, while the bottom boundary of the seabed was fully fixed. The soil was simulated using ten-node tetrahedral elements and the pile using six-node plate elements. The pile was assumed to be 'wished-in-place', and the soil inside the pile was not plugged because the installation process of the pile was ignored.

In order to model the effect of scour protection, two strategies, i.e., the 'stress method' and 'material method', were used in the FEA, as schematically shown in Figure 3. The 'stress method' models the full deviation between the scour protection material and the pile column. Overburden pressure in the vicinity of the pile caused by scour protection layer was implemented by uniformly distributed pressure applied on the seabed in a circular area around the pile., while the 'material method' models full adhesion between the scour protection material and the pile column. The scour protection layer established upon the seabed by the sand of a certain thickness uniformly distributed in a circular area around the

pile. In the real engineering environment, the scour protection material is deviated to the pile column (providing no vertical resistance to the pile due to soil–structure separation), but sometimes, it adheres to the pile column (mobilizing vertical resistance to the pile through soil–structure interaction). Therefore, it was reasonably speculated that the 'stress method' and 'material method' could be regarded as the lower limit and upper limit of the performance of scour protection layer, respectively. In order to explore the difference between the 'stress method' and 'material method' in the modelling the effect of scour protection layer on the vertical bearing behaviour of pile, both of these two modelling strategies were used and the results were compared.

3.2. Material Properties

The Hardening Soil (HS) model [30] available in PLAXIS 3*D* CE V20 was used to model the soil behaviour. The eight material parameters (i.e., c'_{ref}, $\varphi\prime$, ψ, m, E_{50}^{ref}, E_{oed}^{ref}, E_{ur}^{ref}, ν'_{ur}) related with the HS model were firstly derived based on the known relative density of sand from the empirical formulas reported by Brinkgreve et al. [31]. The soil model between the FEA and centrifuge experiments had been calibrated. The calibrated mode parameters for the sand are summarised in Table 3, and the calibration outcome is shown later in Section 4.3. The pile geometry in the FEA was kept identical with that in centrifuge tests. The material behaviour of the pile was assumed to be linear elastic with the parameters E = 210 GPa (Young's modulus) and ν = 0.3 (Poisson's ratio) for steel.

Table 3. Parameters for the HS model.

Parameter	Name	Brinkgreve et al. [25]	After Calibration	Unit
Unit weight	γ	18.2	15.57 (real value)	[kN/m^3]
(Effective) cohesion	c'_{ref}	0 (pre-defined)	0 (pre-defined)	[kN/m^2]
(Effective) angle of internal friction	$\varphi\prime$	38	34 (real value)	[°]
Angle of dilation	ψ	8	4 (real value)	[°]
Secant stiffness for CD triaxial test	E_{50}^{ref}	4.8×10^4	1.6×10^4	[kN/m^2]
Tangent oedometer stiffness	E_{oed}^{ref}	4.8×10^4	1.6×10^4	[kN/m^2]
Unloading reloading stiffness	E_{ur}^{ref}	1.44×10^5	4.8×10^4	[kN/m^2]
Power of stress-level dependency of stiffness	m	0.45	0.45	[-]
Poisson's Ratio for unloading–reloading	ν'_{ur}	0.2	0.2	[-]
Reference stress for stiffness	p^{ref}	100	100	[kN/m^2]
Failure ratio	R_f	0.9	0.9	[-]
K_0—value for normal consolidation	K_0^{nc}	0.4408	0.4408	[-]

3.3. Parametric Case Studies

To identify the effect of scour protection geometries on the vertical loading behaviour of the pile and keep consistency with centrifuge tests, four scour protection widths (i.e., P_w/D = 1, 2, 3, 4) and three scour protection thicknesses (i.e., P_t = 1, 2, 3 m) were established. The scour protection material had a unit weight of 15 kN/m^3. Notably, in the 'stress method' modelling, the scour protection thickness was substituted by equivalent scour protection pressure (i.e., $P_{t,\,equ}$ = 15, 30, 45 kPa), the same as the pressure generated by the overlying scour protection layer in the 'material method' modelling. With the intention of ensuring consistency with centrifuge tests, the influence of water was excluded in this investigation; therefore, both the seabed and the scour protection layer were considered to be dry.

The FEA calculations were executed in several phases. Firstly, the initial stress state in the system caused by the self-weight of the soil was generated using soil elements only.

Subsequently, the monopile was activated and 'wished in place'. Then, scour protection was created, either by activating the overburden pressure in the designed area or the material elements of the designed scour protection geometry. Lastly, a vertical load was applied and increased step by step according to proper loading intervals. A complete FEA programme is presented in Table 4.

Table 4. FEA programme.

Test ID	Methodology	Pile Slenderness (*L*/*D*)	Scour Protection Width	Scour Protection Pressure/Thickness
FEA-0	-	5	-	-
FEA-1	Stress method	5	1*D*	15/30/45 kPa
FEA-2	Stress method	5	2*D*	15/30/45 kPa
FEA-3	Stress method	5	3*D*	15/30/45 kPa
FEA-4	Stress method	5	4*D*	15/30/45 kPa
FEA-5	Material method	5	1*D*	1/2/3 m
FEA-6	Material method	5	2*D*	1/2/3 m
FEA-7	Material method	5	3*D*	1/2/3 m
FEA-8	Material method	5	4*D*	1/2/3 m

4. Interpretation of Measured and Computed Results

All results (measured and computed) reported in the following sections are in prototype scale unless stated otherwise.

4.1. Influence of Scour Protection on Vertical Load–Vertical Displacement Relationships

Figure 4 presents the simulation results of the relationship between the vertical load and vertical displacement under different scour protection widths using the 'stress method' (signified with 'pressure, kPa') and 'material method' (signified with 'thickness, m'). As can be seen from the figure, a nonlinear vertical load–vertical displacement response was observed, and non-linearity became relieved at higher scour protection pressure and thickness. At the same vertical displacement, the vertical load increased proportionally with the increase in scour protection pressure and thickness; although, the higher the scour protection pressure, the larger the initial vertical displacement of the pile (due to the settlement of the seabed caused by applying scour protection measure). Evidently, this phenomenon became more evident with the enlargement of the scour protection width from 1*D* to 4*D*.

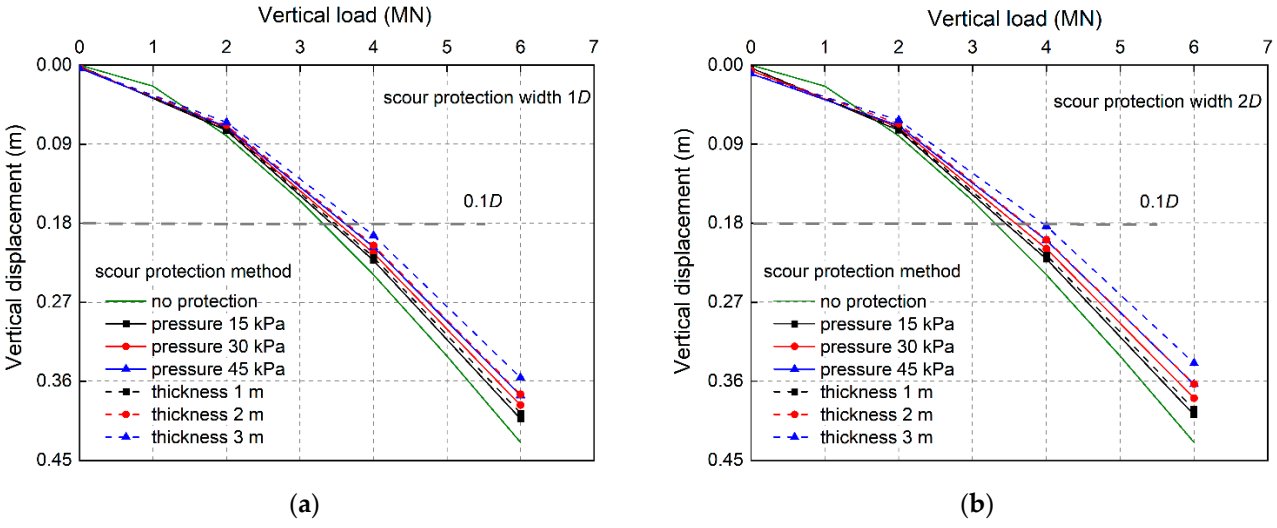

Figure 4. *Cont.*

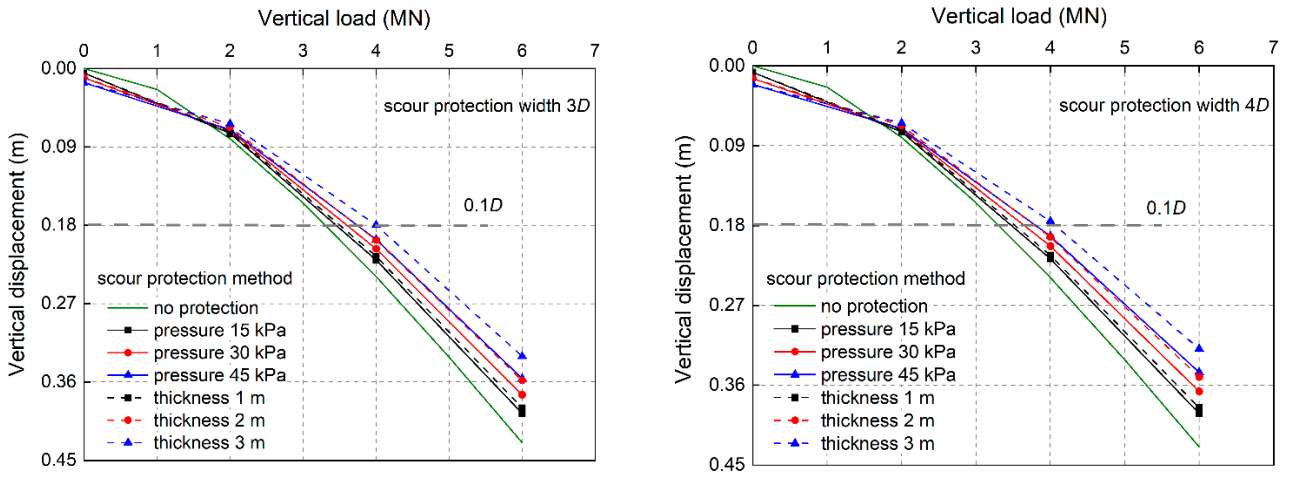

Figure 4. Vertical load–vertical displacement relationships at different scour protection widths: (**a**) 1*D*, (**b**) 2*D*, (**c**) 3*D* and (**d**) 4*D*.

As shown in Figure 4, although the added pressure to the subsoil was the same between the 'material method' and 'stress method', the pile under the 'material method' exhibited higher vertical resistance than the 'stress method'. The difference became more significant with the increase in the scour protection width, scour protection thickness and pressure. In the 'material method', the added scour protection layer played a role of enlarging the pile embedment length, which was assumed to be the main reason for the higher vertical resistance than that in the 'stress method'.

To provide an intuitive insight into the effect of the scour protection width on the vertical load–vertical displacement behaviour of the pile, the same information shown in Figure 4 displayed using the 'stress method' is rearranged and plotted in Figure 5. At the same vertical displacement, the vertical load increased with the increase in scour protection width, which became more evident with the enlargement of the scour protection pressure from 15 kPa to 45 kPa. When the scour protection width was 1*D*, the vertical load was most significantly increased, which illustrates that scour protection functions most efficiently on vertical resistance within the 1*D* area around the pile.

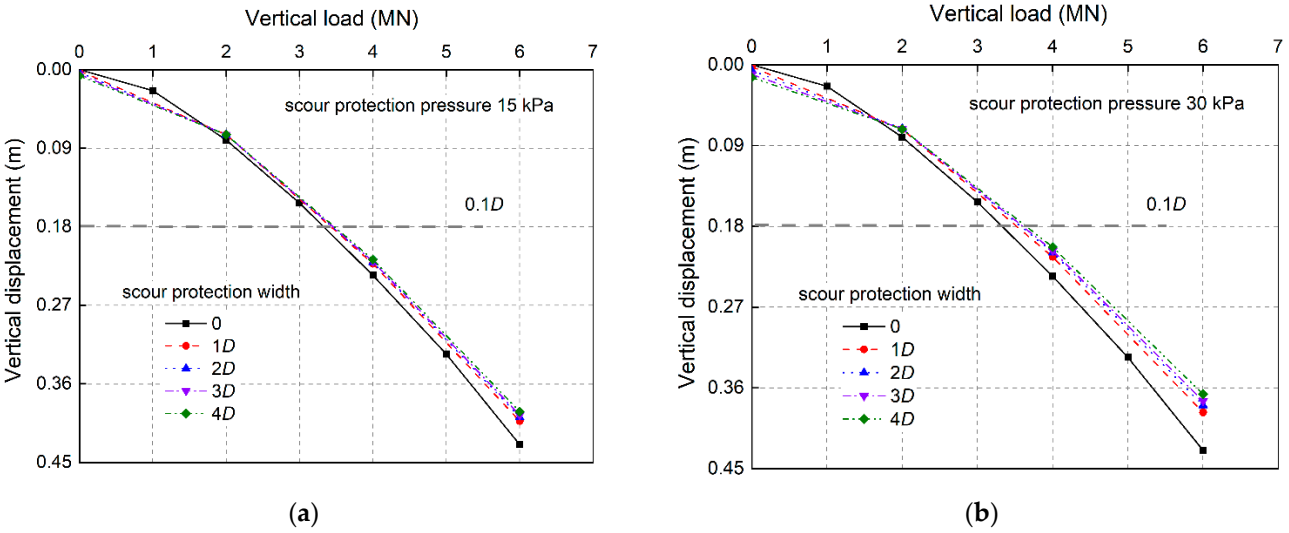

Figure 5. *Cont.*

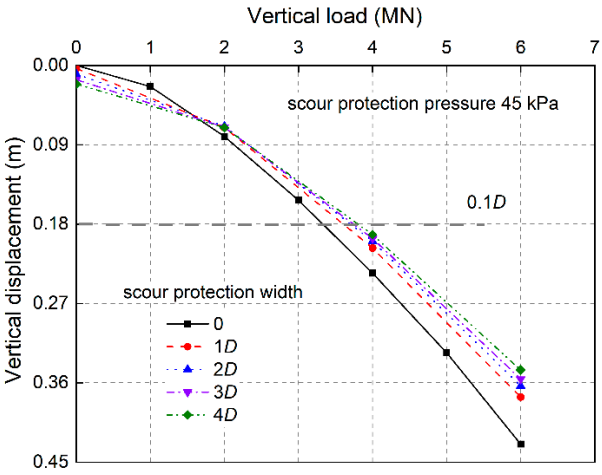

(**c**)

Figure 5. Vertical load–vertical displacement relationships at different scour protection pressures using 'stress method': (**a**) 15 kPa, (**b**) 30 kPa and (**c**) 45 kPa.

4.2. Influence of Scour Protection on Vertical Capacity

The pile vertical capacity (V_{ult}) under various scour protection conditions was defined as the vertical load corresponding to vertical displacement of 0.1D (0.18 m), which could be obtained from Figure 4.

In summary, scour protection could improve the vertical capacity of the pile under all of the investigated scour protection conditions, i.e., scour protection pressures and thicknesses and scour protection widths. Thus, the effect of scour protection on the vertical loading behaviour of the pile could be evaluated using the Vertical Capacity Increase Ratio g_s and g_m (increased vertical capacity under scour protection, t_s and t_m, divided by the vertical capacity under no scour protection, t_0; the subscript s signifies the 'stress method', while the subscript m signifies the 'material method').

Figure 6 shows Vertical Capacity Increase Ratio g_s and g_m considering the influence of the scour protection pressure and thickness and scour protection width using the 'stress method' (signified with 'pressure, kPa') and 'material method' (signified with 'thickness, m'). It can be seen from the figure that Vertical Capacity Increase Ratio g_s and g_m increased with the scour protection pressure and thickness and scour protection width. Under any of the scour protection widths (Figure 6a), g_s and g_m increased almost linearly with the increase in scour protection pressure and thickness.

Overall, the pile Vertical Capacity Increase Ratio under the 'material method' (g_m) had a similar trend with the 'stress method' (g_s) but with a higher value. At a scour protection width of 2D, when the applied scour protection thickness was 1 m, 2 m and 3 m in the 'material method', the Vertical Capacity Increase Ratio g_m, respectively, increased by 0.056, 0.114 and 0.173, compared with that in the 'stress method', where g_s, respectively, increased by 0.054, 0.087 and 0.122. The Vertical Capacity Increase Ratio in the 'material method' (g_m) was 0.2%, 2.7% and 5.1% larger than that in the 'stress method' (g_s), which was very remarkable.

Under any of the applied scour protection pressures and thicknesses (Figure 6b), the pile Vertical Capacity Increase Ratio g_s and g_m increased almost linearly with the increase in the scour protection width. The larger the scour protection pressure and thickness, the larger the Vertical Capacity Increase Ratio g_s and g_m. The initial application of the scour protection width 1D led to the most significant increase in pile Vertical Capacity Increase Ratio g_s and g_m. For example, under a scour protection pressure of 30 kPa, the Vertical Capacity Increase Ratio g_s increased by 0.076, 0.087, 0.098 and 0.115 when the scour protection width 1D, 2D, 3D and 4D was applied. With a scour protection thickness of 2 m, the Vertical Capacity Increase Ratio g_m increased by 0.095, 0.114, 0.125 and 0.139 when

the scour protection width 1*D*, 2*D*, 3*D* and 4*D* was applied. Overall, the scour protection pressure and thickness show a greater impact than the scour protection width on the Vertical Capacity Increase Ratio.

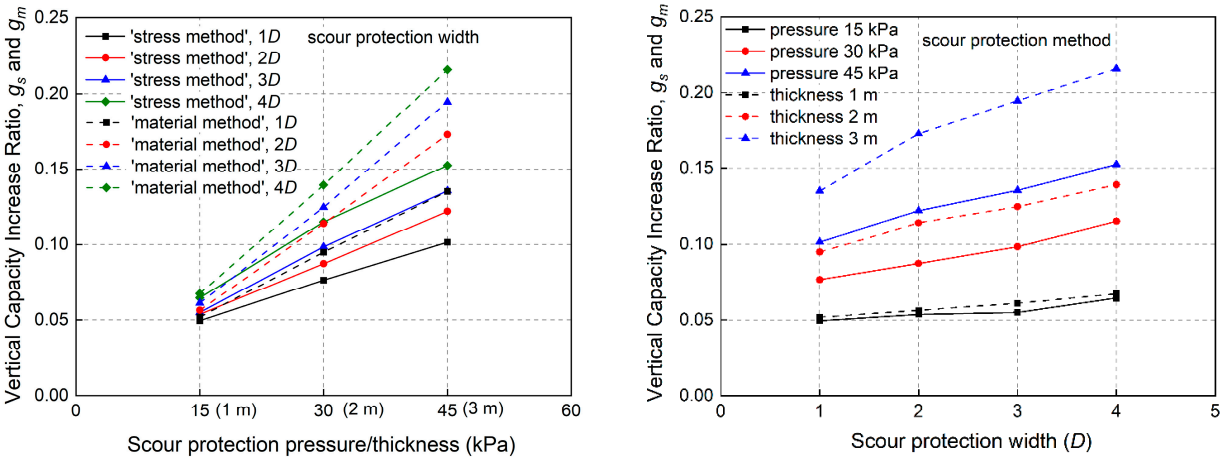

Figure 6. Vertical Capacity Increase Ratio g_s and g_m considering the influence of: (**a**) scour protection pressure and thickness and (**b**) scour protection width.

The validated FEA model is a useful tool to reveal the mechanism of the beneficial contribution from scour protection on vertical loading behaviour of monopiles. Figure 7a,b,d,f,h,j,l present the mean effective stress (σ_m) before and after the application of scour protection pressure using the 'stress method'. Comparing Figure 7a,b,f,j,l, with the increase in scour protection width, the mean effective stress under the protected area increased by around 4%. Comparing Figure 7f,l, increasing the diameter of scour protection from 2*D* to 4*D* had little influence on the enhancement of the mean effective stress in the vicinity of the pile, but it only induced a larger impacted area.

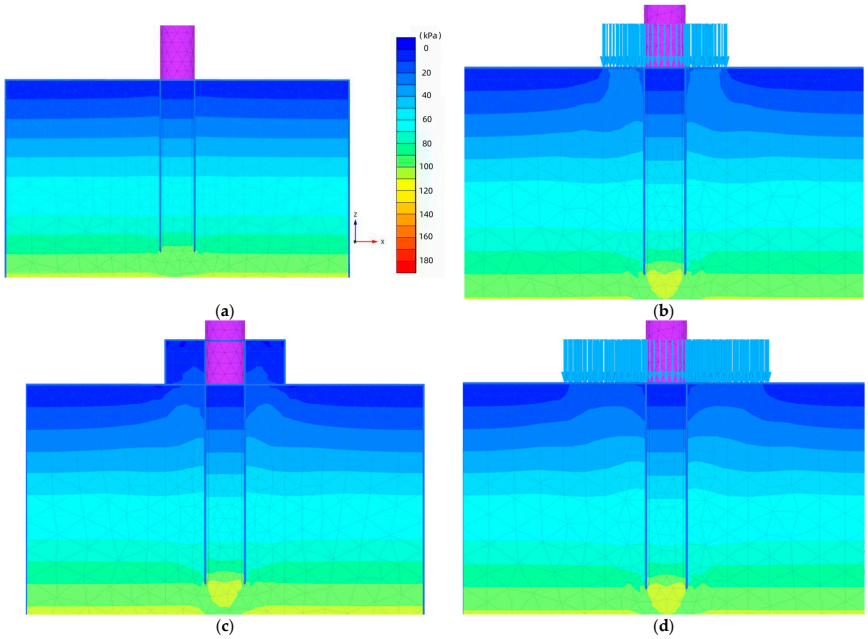

Figure 7. *Cont.*

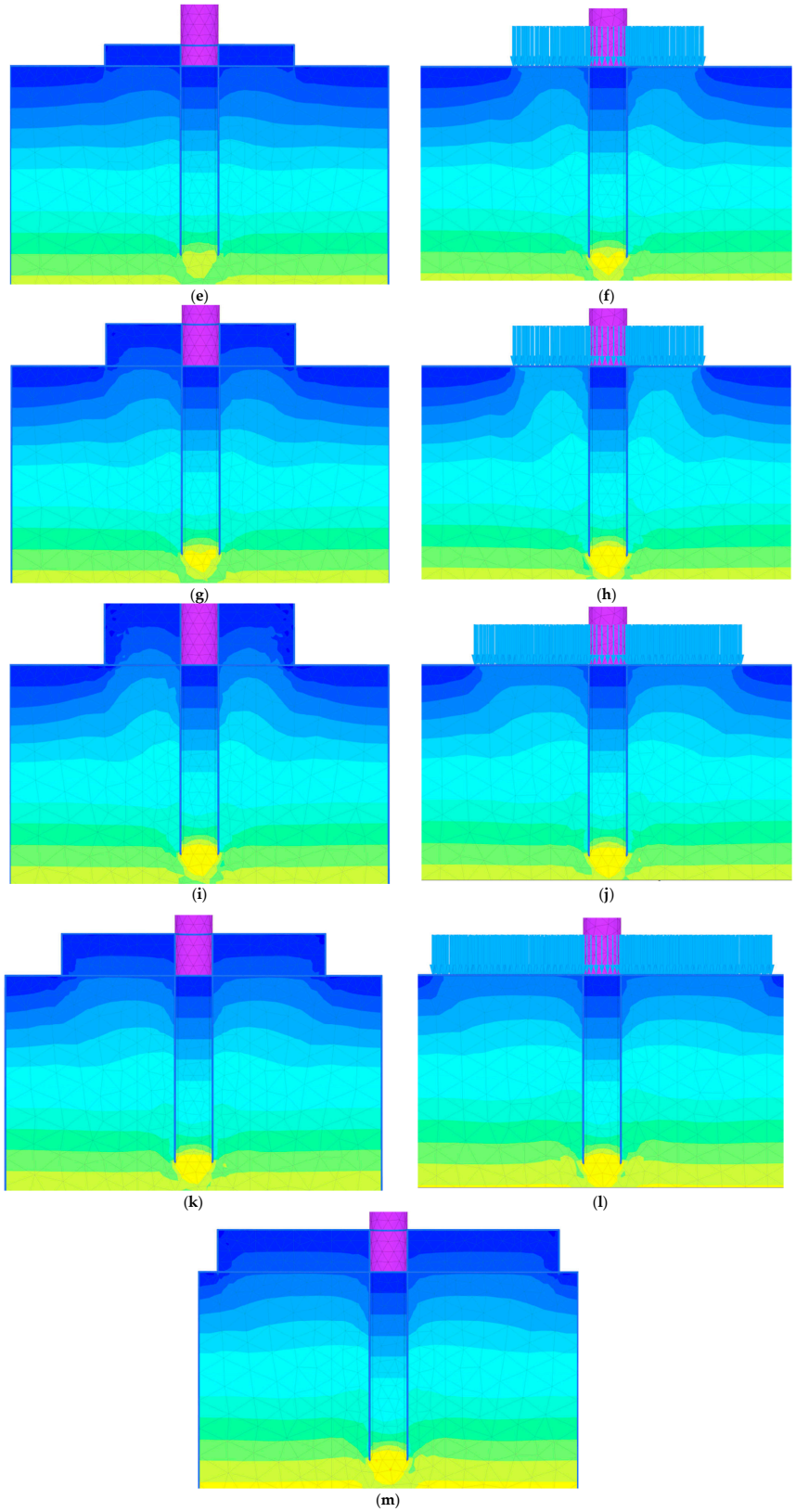

Figure 7. The mean effective stress (σ_m) in the seabed before and after applying scour protection. Note: (**b**,**d**,**f**,**h**,**j**,**l**), 'stress method'; (**c**,**e**,**g**,**i**,**k**,**m**), 'material method'. (**a**) P_w = 0, P_t = 0; (**b**) P_w = 1D, P_t = 30 kPa; (**c**) P_w = 1D, P_t = 2 m; (**d**) P_w = 2D, P_t = 15 kPa; (**e**) P_w = 2D, P_t = 1 m; (**f**) P_w = 2D, P_t = 30 kPa; (**g**) P_w = 2D, P_t = 2 m; (**h**) P_w = 2D, P_t = 45 kPa; (**i**) P_w = 2D, P_t = 3 m; (**j**) P_w = 3D, P_t = 30 kPa; (**k**) P_w = 3D, P_t = 2 m; (**l**) P_w = 4D, P_t = 30 kPa; (**m**) P_w = 4D, P_t = 2 m. Figures share the same legend.

Comparing Figure 7d,f,h, with the increase in scour protection pressure from 15 kPa to 30 kPa to 45 kPa, the mean effective stress under the protected area, respectively, increased by 2%, 4% and 6%, explaining the increase in the vertical capacity, as shown in Figures 4 and 6.

Figure 7c,e,g,i,k,m present the mean effective stress (σ_m) after the application of the scour protection thickness in the 'material method'. Comparing the 'material method' and 'stress method', the influence area and effect of scour protection on the mean effective stress of the substratum soil was very much similar between the two strategies. The added scour protection material directly provided vertical resistance to the pile column, which was why the vertical capacity of the pile increased more significantly.

4.3. Integration of 'Stress Method' and 'Material Method' in Evaluation of Scour Protection Effect on Pile Vertical Loading Behaviour

Based on the FEA performed, compared with the 'stress method', the 'material method' contributed more to the vertical resistance of the pile under the action of the scour protection material. Neither no material contact ('stress method') nor full material contact ('material method') is realistic to accurately evaluate the benefit of scour protection on the vertical resistance of the pile from the perspective of engineering applications.

The 'material method' simulates an ideal case in which the scour protection layer is fabricated perfectly according to the design. However, in the actual construction process of the scour protection layer, stone, gravel and sand are disorganized, and gaps appear between the scour protection material and the pile, due to difficulties in controlling the harsh marine environment.

Therefore, the contact coefficient δ in the 'material method' was introduced to describe the contact effectiveness of the scour protection layer with the pile structure. The value of δ varied between 0 and 1. δ = 0 signifies no material contact, which is equal to the 'stress method'; whereas δ = 1 signifies full material contact, which is equal to the 'material method'. Depending on the actual contact between the scour protection layer and pile column, the designer could make choice of a realistic δ value.

Then, the actual vertical capacity of the pile under scour protection can be expressed as

$$t_{ac} = t_0 \times (1 + g_s + \delta \times \eta) = t_0 \times [1 + g_s + \delta \times (g_m - g_s)] \quad (1)$$

where t_{ac} denotes the actual vertical capacity under scour protection, t_0 denotes the vertical capacity without scour protection, g_s denotes the Vertical Capacity Increase Ratio by the 'stress method' and g_m denotes the Vertical Capacity Increase Ratio by the 'material method'. The vertical reinforcement factor η ($\eta = g_m - g_s$) describes the extra enhancement of the Vertical Capacity Increase Ratio by the 'material method' compared with the 'stress method'. The η values under the investigated scour protection conditions are given in Table 5.

Table 5. Vertical reinforcement factor, η.

Scour Protection Width	Scour Protection Thickness/Pressure			Average
	1 m/15 kPa	2 m/30 kPa	3 m/45 kPa	
1*D*	0.002	0.018	0.034	0.018
2*D*	0.003	0.027	0.051	0.027
3*D*	0.006	0.026	0.059	0.030
4*D*	0.003	0.024	0.063	0.030
Average	0.004	0.024	0.052	0.026

As shown in Table 5, the vertical reinforcement factor η basically remained constant with the increase in the scour protection width, but showed an upward trend with the increase in the scour protection thickness and pressure. Under all of the investigated scour protection conditions, η had an average value of 0.026, which means the vertical capacity

of the pile simulated under the 'material method' was 2.6% larger than that of the pile simulated under the 'stress method'. However, under small scour protection thickness and pressure (1 m/15 kPa, specifically), η had an average value of 0.004, implying a non-significant difference in the increase in the vertical capacity brought by scour protection between the 'material method' and 'stress method'. Under large scour protection thickness and pressure (3 m/45 kPa, specifically), η had an average value of 0.052, which was very remarkable. Therefore, concern should be placed on the cost-effective design of monopiles when evaluating the effect of scour protection on the vertical capacity of the pile, especially under large scour protection thickness and pressure.

The vertical load–vertical displacement relationships measured from centrifuge tests (CT-1, CT-2 and CT-3) and the FEA (FEA-0; FEA-2, FEA-3 under scour protection pressure of 15 kPa; FEA-6, FEA-7 at scour protection thickness of 1 m) are presented in Figure 8. It can be seen from the figure that the FEA model well captured the overall development of vertical displacement with vertical load for the centrifuge test without scour protection, which proves the reliability of the calibrated material parameters of the HS model. Comparing the vertical load–vertical displacement relationships for centrifuge tests with a scour protection width 2*D* and without scour protection, the vertical capacity of the pile foundation increased by a maximum of 7%. When the scour protection width was raised from 2*D* to 3*D*, the overall vertical load–vertical displacement relationship changed by about 2%. The vertical resistance of the pile under scour protection conditions was generally stronger in centrifuge tests than that in the FEA.

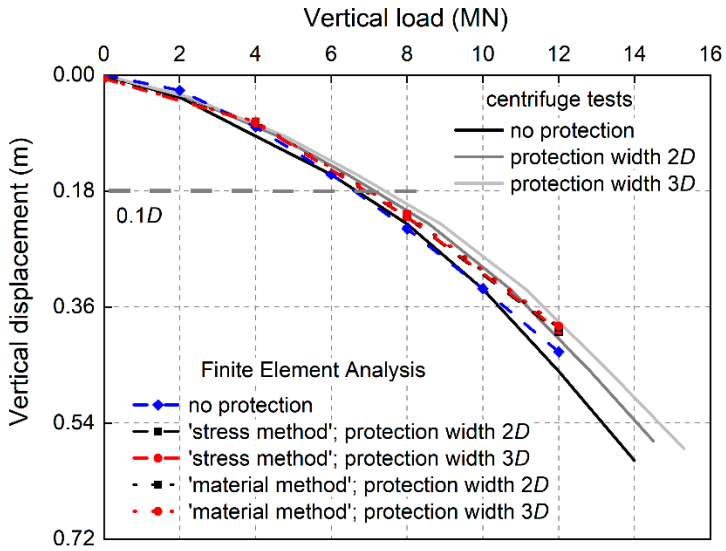

Figure 8. Vertical load–vertical displacement relationships compared between centrifuge tests and FEA.

4.4. Designing Example

An example is given to demonstrate the use of the proposed Equation (1) in calculating the actual vertical capacity of the pile under scour protection conditions, considering a rigid monopile, with L/D = 5, embedded in sand with a relative density of 80%. The task is to determine the pile actual vertical capacity (t_{ac}) under a scour protection thickness of P_t = 1.6 m and scour protection width of P_w = 2.2*D*, when assuming the 'material method' contact coefficient of δ = 0.6. The scour protection material had a unit weight of γ = 14 kN/m^3. Under certain design conditions, the vertical capacity of the monopile without scour protection was pre-determined to be t_0 = 6 MN.

Firstly, we converted the scour protection thickness P_t (=1.6 m) to the equivalent scour protection pressure $P_{t,\,equ}$ as follows:

$$P_{t,\,equ} = \gamma \times P_t = 14 \times 1.6 = 22.4 \text{ kPa} \quad (2)$$

With the equivalent scour protection pressure (22.4 kPa) and scour protection width (2.2D), the Vertical Capacity Increase Ratio g_s of the pile (by the 'stress method') was calculated to be 0.071 using the interpolation method according to Figure 6b. The vertical reinforcement factor η was calculated to be 0.015 using the interpolation method according to Table 5.

Accordingly, the actual vertical capacity (t_{ac}) of the pile was calculated according to Equation (1):

$$t_{ac} = t_0 \times (1 + g_s + \delta \times \eta) = 6 \times (1 + 0.071 + 0.6 \times 0.015) = 6 \times 1.08 = 6.48 \text{ MN} \quad (3)$$

In summary, by applying the scour protection measures, the vertical capacity of the pile increased by 8% to 6.48 MN, which may satisfy the need of substituting a new structure.

5. Conclusions

A series of centrifuge tests and Finite Element Analyses were performed in this study to investigate the influence of scour protection on the vertical loading behaviour of monopiles. The following conclusions can be drawn:

1. Scour protection can increase the vertical capacity of the pile. At a scour protection width of 2D and an applied scour protection pressure of 30 kPa, the vertical capacity of the pile increases by 8% compared with that in the absence of scour protection.
2. The scour protection material can not only provide the subsoil overburden pressure but also directly create vertical resistance to the pile structure. By using the 'material method', the added protection material plays a role in enlarging the embedment length of the pile, making the Vertical Capacity Increase Ratio under the 'material method' about 2.6% larger than that obtained using the 'stress method'.
3. The contact coefficient δ in the 'material method' could be incorporated into the design methodology of the pile to reflect and compare the effectiveness in increasing the vertical capacity between the 'material method' and 'stress method'. The centrifuge tests and FEA results show good agreement, which proves the reliability of calibrated material parameters of the HS model.

Though a small pile has been simulated in this research, the analysis methodology and calculation results could provide useful guidance on the analysis of similar projects and problems.

6. Limitations

Both centrifugal and numerical methodologies in this research follow the 'pile installation-scour protection formation' procedure, and the later step happens instantly after the former one. The corresponding project background is that scour protection measures are activated soon after the pile installation. However, in some of the engineering applications, scour protection is applied as a remedial measure for recovering pile resistance. Under this circumstance, the pile foundation has already been in the working state for a long time, and thus, the influence of scour protection on the vertical resistance behaviour of the pile is different from that in this research.

Most of the monopile foundations are installed in the marine environment, where the cementation effect may occur, thus affecting interparticle contact properties, changing the roughness of the pile outer surface and influencing the soil–structure interaction and the loading behaviour of the pile. The effect of aging on the vertical bearing resistance of the pile is complicated and causes ambiguity on the influence of scour protection on the vertical capacity. These two effects could be explored using laboratory experiments in order to better understand the variation in the vertical resistance behaviour of the pile over time, especially when structures are submerged in salt water. Further study is encouraged to explore the influence of scour protection on the vertical loading behaviour of the pile considering combined lateral cyclic loading.

Author Contributions: Conceptualization, Q.L., X.W. and K.G.; methodology, Q.L. and K.G.; software, Q.L. and H.D.; investigation, Q.L. and K.W.; writing—original draft preparation, Q.L. and H.D.; writing—review and editing, X.W. and K.W.; supervision, X.W. and K.G.; funding acquisition, X.W., K.G. and S.J.; validation, S.J. All authors have read and agreed to the published version of the manuscript.

Funding: National Natural Science Foundation of China (NSFC) (Grant No. 52278373 and No. 52009122), Zhejiang Provincial Natural Science Foundation of China (Grant No. LQ21E090002), and Zhejiang Engineering Research Centre of Intelligent Urban Infrastructure (IUI2022-ZD-01 and IUI2023-ZD-02). China Scholarship Council (CSC). Section of Geo-Engineering, Delft University of Technology.

Data Availability Statement: Data will be available on request.

Acknowledgments: The authors would like to acknowledge the support of the Section of Civil Engineering, Hangzhou City University, the Section of Geo-Engineering, Delft University of Technology, and the funding from the CSC.

Conflicts of Interest: Author Qiang Li was employed by PowerChina Huadong Engineering (Shenzhen) Corporation Limited, and Shengxiang Jiang was employed by the company PowerChina Huadong Engineering Corporation Limited. The remaining authors declare that the research was conducted in the absence of any commercial or financial relationships that could be construed as a potential conflict of interest.

List of Notation

C_U	uniformity coefficient of sand	p^{ref}	reference stress for stiffness
c'_{ref}	(effective) cohesion	P_t	scour protection thickness
D	pile outer diameter	$P_{t,\ equ}$	equivalent scour protection pressure
D_{50}	average grain size of sand	P_w	scour protection width
D_r	relative density of sand	R_f	failure ratio
D_s	scour depth	t	pile wall thickness
E	Young's modulus	t_{ac}	actual vertical capacity under scour protection
E_{50}^{ref}	secant stiffness for CD triaxial test	t_0	vertical capacity without scour protection
E_{oed}^{ref}	tangent oedometer stiffness	V	vertical load
E_{ur}^{ref}	unloading reloading stiffness	γ	unit weight of sand
e	loading eccentricity	δ	'material method' contact coefficient
e_{max}	maximum void ratio of sand	ψ	angle of dilation
e_{min}	minimum void ratio of sand	η	vertical reinforcement factor
g	gravitational acceleration rate	φ'	(effective) angle of internal friction
g_m	Vertical Capacity Increase Ratio by 'material method'	ν	Poisson's ratio
g_s	Vertical Capacity Increase Ratio by 'stress method'	ν'_{ur}	Poisson's ratio for unloading–reloading
h	water depth	FEA	Finite Element Analysis
K_0^{nc}	K_0—value for normal consolidation	HS	Hardening Soil
L	pile embedded length	OWT	Offshore Wind Turbine
m	power of stress-level dependency of stiffness		

References

1. Komusanac, I.; Brindley, G.; Fraile, D.; Ramirez, L. Wind Energy in Europe. In *2021 Statistics and the Outlook for 2022–2026*; Technical report; Wind Europe: Brussels, Belgium, 2022. Available online: https://www.anev.org/wp-content/uploads/2022/02/220222-Stats-Outlook.pdf (accessed on 8 November 2023).
2. Topham, E.; Gonzalez, E.; McMillan, D.; João, E. Challenges of decommissioning offshore wind farms: Overview of the Eu-ropean experience. *J. Phys. Conf. Ser.* **2019**, *1222*, 012035. [CrossRef]
3. Kerkvliet, H.; Polatidis, H. Offshore wind farms' decommissioning: A semi quantitative Multi-Criteria Decision Aid framework. *Sustain. Energy Technol. Assess.* **2016**, *18*, 69–79. [CrossRef]
4. Ortegon, K.; Nies, L.F.; Sutherland, J.W. Preparing for end of service life of wind turbines. *J. Clean. Prod.* **2013**, *39*, 191–199. [CrossRef]
5. Nielsen, A.W.; Liu, X.; Sumer, B.M.; Fredsøe, J. Flow and bed shear stresses in scour protections around a pile in a current. *Coast. Eng.* **2013**, *72*, 20–38. [CrossRef]
6. Petersen, T.U.; Sumer, B.M.; Fredsøe, J.; Raaijmakers, T.C.; Schouten, J.-J. Edge scour at scour protections around piles in the marine environment—Laboratory and field investigation. *Coast. Eng.* **2015**, *106*, 42–72. [CrossRef]
7. Sumer, B.M.; Fredsøe, J.; Christiansen, N. Scour Around Vertical Pile in Waves. *J. Waterw. Port Coast. Ocean Eng.* **1992**, *118*, 15–31. [CrossRef]
8. Li, Q.; Prendergast, L.J.; Askarinejad, A.; Chortis, G.; Gavin, K. Centrifuge Modeling of the Impact of Local and Global Scour Erosion on the Monotonic Lateral Response of a Monopile in Sand. *Geotech. Test. J.* **2020**, *43*, 1084–1100. [CrossRef]
9. Lin, C.; Bennett, C.; Han, J.; Parsons, R.L. Scour effects on the response of laterally loaded piles considering stress history of sand. *Comput. Geotech.* **2010**, *37*, 1008–1014. [CrossRef]
10. Qi, W.G.; Gao, F.P.; Randolph, M.F.; Lehane, B.M.; Amini, S.A.; Mohammad, T.A.; Aziz, A.A.; Ghazali, A.H.; Huat, B.B.K.; Day, R.A.; et al. Scour effects on *p–y* curves for shallowly embedded piles in sand. *Géotechnique* **2016**, *66*, 648–660. [CrossRef]
11. Askarinejad, A.; Wang, H.; Chortis, G.; Gavin, K. Influence of scour protection layers on the lateral response of monopile in dense sand. *Ocean Eng.* **2021**, *244*, 110377. [CrossRef]
12. Li, Q.; Askarinejad, A.; Gavin, K. Impact of scour on lateral resistance of wind turbine monopiles: An experimental study. *Can. Geotech. J.* **2021**, *58*, 1770–1782. [CrossRef]
13. Zhang, W.; Askarinejad, A. Centrifuge modelling of submarine landslides due to static liquefaction. *Landslides* **2019**, *16*, 1921–1938. [CrossRef]
14. Doherty, P.; Gavin, K. Laterally loaded monopile design for offshore wind farms. *Proc. Inst. Civ. Eng. Energy* **2012**, *165*, 7–17. [CrossRef]
15. Wu, X.; Hu, Y.; Li, Y.; Yang, J.; Duan, L.; Wang, T.; Adcock, T.; Jiang, Z.; Gao, Z.; Lin, Z.; et al. Foundations of offshore wind turbines: A review. *Renew. Sustain. Energy Rev.* **2019**, *104*, 379–393. [CrossRef]
16. Li, Q.; Gavin, K.; Askarinejad, A.; Prendergast, L.J. Experimental and numerical investigation of the effect of vertical loading on the lateral behaviour of monopiles in sand. *Can. Geotech. J.* **2022**, *59*, 652–666. [CrossRef]
17. Byrne, B.W.; MCadam, R.; Burd, H.J.; Houlsby, G.T.; Martin, C.M.; Gavin, K.; Doherty, P.; Igoe, D.; Zdravkovie, L.; Taborda, D.M.G.; et al. Field testing of large diameter piles under lateral loading for offshore wind applications. In Proceedings of the XVI ECSMGE Geotechnical Engineering for Infrastructure and Development, Edinburgh, Scotland, 13–17 September 2015; pp. 1255–1260.
18. Byrne, B.W.; Burd, H.J.; Zdravković, L.; McAdam, R.A.; Taborda, D.M.; Houlsby, G.T.; Jardine, R.J.; Martin, C.M.; Potts, D.M.; Gavin, K.G. PISA: New design methods for offshore wind turbine monopiles. *Rev. Française Géotechnique* **2019**, *3*, 158. [CrossRef]
19. Li, Q. Response of Monopiles Subjected to Combined Vertical and Lateral Loads, Lateral Cyclic Load, and Scour Erosion in Sand. Ph.D. Thesis, Delft University of Technology, Delft, The Netherlands, 2020. [CrossRef]
20. De Nicola, A. The Performance of Pipe Piles in Sand. Ph.D. Thesis, University of Western Australia, Perth, Australia, 1996.
21. De Nicola, A.; Randolph, M.F. The plugging behaviour of driven and jacked piles in sand. *Géotechnique* **1997**, *47*, 841–856. [CrossRef]
22. Mu, L.; Kang, X.; Feng, K.; Huang, M.; Cao, J. Influence of vertical loads on lateral behaviour of monopiles in sand. *Eur. J. Environ. Civ. Eng.* **2018**, *22*, s286–s301. [CrossRef]
23. Verdure, L.; Garnier, J.; Levacher, D. Lateral Cyclic Loading of Single Piles in Sand. *Int. J. Phys. Model. Geotech.* **2003**, *3*, 17–28.
24. Klinkvort, R.T.; Hededal, O. Lateral Response of Monopile Supporting an Offshore Wind Turbine. *Proc. Inst. Civ. Eng. Geotech. Eng.* **2013**, *166*, 147–158. [CrossRef]
25. Leblanc, C.; Houlsby, G.T.; Byrne, B.W. Response of stiff piles in sand to long-term cyclic lateral loading. *Géotechnique* **2010**, *60*, 79–90. [CrossRef]
26. Li, Z.; Haigh, S.K.; Bolton, M.D. Centrifuge Modelling of Mono-Pile under Cyclic Lateral Loads. In Proceedings of the 7th International Conference on Physical Modelling in Geotechnics, Zurich, Switzerland, 28 June–1 July 2010; Volume 2, pp. 965–970.
27. Du, S. Study on Local Erosion Characteristics and Solidified Soil Protection of Single Pile Foundation for Offshore Wind Power. Master Thesis, Southeast University, Dhaka, Bangladesh, 2021.
28. Matutano, C.; Negro, V.; López-Gutiérrez, J.-S.; Esteban, M.D. Scour prediction and scour protections in offshore wind farms. *Renew. Energy* **2013**, *57*, 358–365. [CrossRef]

29. Lengkeek, W.; Didderen, K.; Teunis, M.; Driessen, F.; Coolen, J.W.P.; Bos, O.G.; Vergouwen, S.A.; Raaijmakers, T.; De Vries, M.B.; Van Koningsveld, M. *Eco-Friendly Design of Scour Protection: Potential Enhancement of Ecological Functioning in Offshore Wind Farms: Towards an Implementation Guide and Experimental Set-Up*; Bureau Waardenburg: Culemborg, The Netherlands, 2017; Volume 96.
30. Schanz, T. Zur Modellierung des Mechanischen Verhaltens von Reibungsmaterialen. Ph.D. Thesis, Stuttgart University, Stuttgart, Germany, 1998. (In German)
31. Brinkgreve, R.B.J.; Engin, E.; Engin, H. Validation of empirical formulas toderive model parameters for sands. In Proceedings of the 7th European Conference Numerical Methods in Geotechnical Engineering, Trondheim, Norway, 2–4 June 2010; Volume 1, pp. 137–174.